ELSEVIER

Blood 142 (2023) 5755–5757

The 65th ASH Annual Meeting Abstracts

ONLINE PUBLICATION ONLY

604.MOLECULAR PHARMACOLOGY AND DRUG RESISTANCE: MYELOID NEOPLASMS

Population Pharmacokinetic and Pharmacodynamic Analysis of Navtemadlin in Patients with Relapsed and Refractory (R/R) Myelofibrosis (MF) and Other Myeloid or Solid Tumor Malignancies

Lu Zhang[1], *Bill Poland*[1], *Shuang Xu*[1], *Martine Allard*[2], *Cecile Krejsa, PhD*[2], *J. Greg Slatter*[2]

[1] Certara Inc., Princeton, NJ
[2] Kartos Therapeutics Inc., Redwood City, CA

Background: Murine double minute 2 (MDM2), a key negative regulator of the tumor suppressor protein p53, is overexpressed in malignancies such as MF and Merkel cell carcinoma (MCC). Navtemadlin is a potent, selective, orally available MDM2 inhibitor that overcomes MDM2 dysregulation by restoring p53 activity and inducing apoptosis of *TP53*^{WT} tumors. Navtemadlin has been tested in 21- or 28-day treatment cycles, with 5 or 7 consecutive days of dosing per cycle.
Navtemadlin elicits plasma concentration-dependent increases in serum macrophage inhibitory cytokine-1 (MIC-1). An increase in MIC-1 relative to baseline MIC-1 serum concentration is a key pharmacodynamic (PD) marker of response to navtemadlin treatment (Zhang et al. *Xenobiotica* 2022).
A population pharmacokinetic (PK) model was developed, based on patients with R/R MF (N=113, NCT03662126); MCC (N=35, NCT03787602); solid tumors and multiple myeloma (ST/MM N=105, Gluck et al. *Invest New Drugs* 2019); R/R acute myeloid leukemia (AML, N=35, Erba et al. *Blood Adv* 2019); and healthy volunteers (HV, N=30, Wong et al. *Clin Pharmacol Drug Dev* 2022).The objectives wereto characterize navtemadlin PK and covariate effects and compare steady-state (SS) PK and PD across cancer types.
Methods:A two-compartment PK model with first-order absorption and elimination was estimated using NONMEM ® (first-order conditional estimation with interaction). Four transit compartments captured absorption. Inter-subject variability was modeled as lognormal. A stepwise covariate search used forward addition ($p<0.05$) followed by backward elimination ($p<0.01$). Log-transformed SS MIC-1 ratio to baseline (fold ratio) was tested in a fixed-effects linear regression model with respect to SS exposures, with baseline MIC-1 as the covariate. The final population PK and MIC-1 models were evaluated by inspection of parameter tables, by overlaying model predictions with observed data, and by standard residual diagnostics.
Results: The PK estimation used 5,282 concentrations from 318 subjects, including 1,415 concentrations in 113 patients with R/R MF. Tumor type affected absorption rate (median, 0.635/hr in MCC; slower vs other types), apparent clearance (median, 8.90 L/hr in MCC; lower vs other types), and apparent central volume (median, 64.4 L in MCC; similar to AML, but lower vs other types) (Table 1). Accordingly, simulated SS area under the curve (AUCss) differed across populations in the order MCC>AML>MF>ST/MM = HV (Figure 1).
Covariate analysis indicated median AUC increased with the inflammation marker C-reactive protein, by 21% at 90 th percentile CRP, and with age, by 5% at 90 th percentile age of 75 y, compared to the median, 66 y. Men had 24% lower relative bioavailability than women. Taking navtemadlin with food slowed absorption by 10% but had no impact on AUCss. Other tested covariates, including body weight, creatinine clearance, aspartate transaminase, alanine transaminase, bilirubin, albumin, alpha 1-acid glycoprotein, race, UGT1A1 genotype, recent ruxolitinib treatment in MF, and CYP3A4 inducer/inhibitor concomitant medications, were not significant.
Median MIC-1 fold ratio increased with navtemadlin AUCss. Higher baseline MIC-1 resulted in lower SS MIC-1 fold ratio. Median baseline MIC-1 differed by tumor type. In R/R MF, baseline MIC-1 was 2,297 ng/L and SS fold ratio of MIC-1 was 7.79 (N=91). In MCC, baseline MIC-1 was 1,718 ng/L and SS fold ratio of MIC-1 was 16.7 (N=29). In R/R MF, higher baseline spleen volume was also associated with lower SS MIC-1 fold ratio. Exposure-MIC-1 relationships in R/R MF and MCC were generally similar to other tumor types and HV populations (Allard et al. *Hemasphere* 2019; Zhang et al. *Xenobiotica* 2022).
Conclusions: Tumor type influenced navtemadlin exposure with simulated exposure in R/R MF patients at the selected Phase 3 dose of 240 mg comparable to exposures in MCC patients at 180 mg, the selected Phase 2 dose for that indication. Cancer-associated inflammation and/or treatment history, as well as age and female sex, may increase navtemadlin exposure. The PD marker MIC-1 responds to navtemadlin in a concentration-dependent fashion. The overall SS fold change of MIC-1 PD

responses was lower in disease states or subjects with higher baseline MIC-1. These studies demonstrate potent, dose-dependent PK/PD responses following p53 activation with the novel MDM2 inhibitor, navtemadlin, across diverse tumor types.

Disclosures Zhang: *Certara Inc.:* Ended employment in the past 24 months; *Kartos Therapeutics:* Consultancy. **Poland:** *Certara Inc.:* Current Employment; *Kartos Therapeutics:* Consultancy. **Xu:** *Certara Inc.:* Current Employment; *Kartos Therapeutics:* Consultancy. **Allard:** *Kartos Therapeutics:* Current equity holder in private company; *Telios Pharma:* Current Employment, Current equity holder in private company. **Krejsa:** *AstraZeneca:* Current equity holder in publicly-traded company, Ended employment in the past 24 months; *Kartos Therapeutics:* Current Employment, Current equity holder in private company, Current holder of *stock options* in a privately-held company; *Seattle Genetics:* Current equity holder in publicly-traded company, Ended employment in the past 24 months; *Acerta Pharma:* Current equity holder in private company, Ended employment in the past 24 months. **Slatter:** *Acerta Pharma:* Current equity holder in private company; *AstraZeneca:* Current equity holder in publicly-traded company; *Kartos Therapeutics:* Current Employment, Current equity holder in private company; *Telios Pharma:* Current equity holder in private company; *Amgen:* Current equity holder in publicly-traded company.

Table 1: Selected Final Navtemadlin Population PK Model Parameter Estimates

Parameter	Description	Estimate	RSE%
Ka (1/h)	Absorption Rate Constant of MCC	0.635	10.5
CL/F (L/h)	Apparent Clearance of MCC	9.26	11.0
Vc/F (L)	Apparent Central Volume of MCC, MF, AML	71.5	7.08
Q/F (L/h)	Apparent Inter-compartmental CL	24.7	8.07
Vp/F (L)	Apparent Peripheral Volume	188.0	7.97
AGE_CL/F	Age on CL/F: (AGE/65)**THETA	−0.417	30.8
CRP_CL/F	CRP on CL/F: (CRP/5)**THETA	−0.114	25.7
MF_CL/F	CL/F of MF: (1+THETA)	0.394	42.7
AML_CL/F	CL/F of AML: (1+THETA)	0.267	66.2
ST/MM CL/F	CL/F of solid Tumor and MM: (1+THETA)	1.32	21.8
HV_CL/F	CL/F of healthy volunteers: (1+THETA)	0.439	52.4
Male_F	Relative Bioavailability of Males (1+THETA)	−0.244	20.0

Figure 1: Simulated Steady-State AUC in MCC and Other Populations After 120, 180, and 240 mg Daily Navtemadlin Dosing

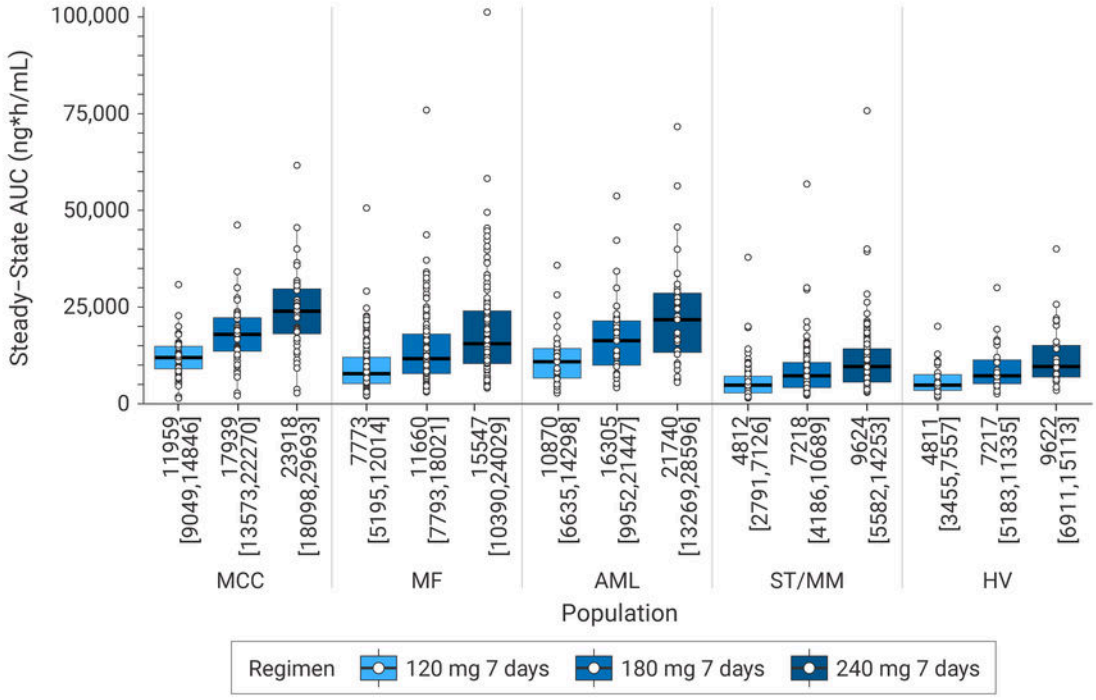

Points are individual post hoc simulations. Numbers below the boxplots are median [25th percentile, 75th percentile]. Abbreviations: AML, acute myeloid leukemia; AUC, area under the curve; HV, healthy volunteers; MCC, Merkel cell carcinoma; MF, myelofibrosis; RSE%, relative standard error x 100%; ST/MM, solid tumors or multiple myeloma.
References: Erba HP et al., *Blood Adv*. 2019;3: 1939-1949. Gluck WL et al., *Invest New Drugs*. 2020;38: 831-843. Wong S et al., *Clin Pharmacol Drug Dev*. 2022;11(5): 640-653.

Figure 1

https://doi.org/10.1182/blood-2023-174749